DOI:
10.1007/s00125-016-4076-3

Document Version
Peer reviewed version

TITLE: eNAMPT-monomer plays an important role in development of experimental diabetes in mice and represents a potential target for treatment of type 2 diabetes

AUTHORS: Julius Kieswich[1], Sophie R. Sayers[2], Marta F. Silvestre[3,4] Steven M. Harwood[1], Muhammad M. Yaqoob[1], Paul W. Caton[2]

[1] Translational Medicine and Therapeutics, William Harvey Research Institute, Bart's and the London School of Medicine and Dentistry, Queen Mary University of London, UK;

[2]Diabetes Research Group, Division of Diabetes and Nutritional Sciences, King's College London, UK

[3]Faculdade de Medicina da Universidade de Lisboa, Lisboa, Portugal;

[4]Human Nutrition Unit, University of Auckland, New Zealand;

Corresponding Author: Paul W. Caton, Division of Diabetes and Nutritional Sciences, King's College London, Hodgkin Building, Guy's Campus, London, SE1 1UL; TEL: +44 (0) 207 848 6436; Email, paul.w.caton@kcl.ac.uk.

Abstract: 249 words

Main text: 3812

Abstract

Aims/Hypothesis Serum extra-cellular nicotinamide phosphoribosyltransferase (eNAMPT) concentrations are elevated in type 2 diabetes. However, the relationship between abnormally elevated serum eNAMPT and type 2 diabetes pathophysiology is unclear. eNAMPT circulates in functionally and structurally distinct monomer and dimer forms. eNAMPT-dimer exerts NAD-biosynthetic activity. The role of eNAMPT-monomer is unclear but may exert NAD-independent pro-inflammatory effects. However studies of eNAMPT in type 2 diabetes have not distinguished between monomer and dimer forms. Since type 2 diabetes is characterised by chronic inflammation, we hypothesised a selective role for NAD-independent eNAMPT-monomer in type 2 diabetes.

Methods Two models were used to examine the role of eNAMPT-monomer in type 2 diabetes; (A) diabetic high-fat fed mice (HFD; 10 weeks) were administered (I.P.) anti-eNAMPT-monomer antibody; (B) lean non-diabetic mice were administered recombinant eNAMPT-monomer daily (14 days; I.P.)

Results Serum eNAMPT-monomer levels were elevated in diabetic HFD mice, whilst eNAMPT-dimer levels were unchanged. eNAMPT-monomer neutralization in HFD mice resulted in lowered blood glucose, amelioration of impaired glucose tolerance (IGT) and whole-body insulin resistance, improved pancreatic islet function and reduced inflammation. These effects were maintained at least 3 weeks post-dosing. eNAMPT-monomer administration induced a diabetic phenotype in mice, characterised by elevated blood glucose, IGT, impaired pancreatic insulin secretion and presence of systemic and tissue inflammation, without changes in NAD levels.

Conclusions/Interpretations We demonstrate that elevation of eNAMPT-monomer plays an important role in the pathogenesis of diet-induced diabetes, via pro-inflammatory mechanisms. These data provide proof-of-concept evidence that eNAMPT-monomer represents a potential therapeutic target for type 2 diabetes.

Key Words: extra-cellular nicotinamide phosphoribosyltransferase; eNAMPT; beta-cell; islet; type 2 diabetes, inflammation

Abbreviations

ADGRE1	adhesion G protein-coupled receptor E1
CCL2	Chemokine (C-C Motif) Ligand 2
IGT	Impaired glucose tolerance
IPGTT	intra-peritoneal glucose tolerance test
iNAMPT	intra-cellular nicotinamide phosphoribosyltransferase
eNAMPT	extracellular nicotinamide phosphoribosyltransferase
GSIS	glucose-stimulated insulin secretion
FASN	fatty acid synthase
HFD	high-fat diet
HOMA-IR	homeostatic model assessment of insulin resistant
HPLC	high performance liquid chromatography
ITGAM	Integrin, Alpha M (Complement Component 3 Receptor 3 Subunit)
ITGAX	Integrin, alpha X (complement component 3 receptor 4 subunit)
iNAMPT	intracellular nicotinamide phosphoribosyltransferase
IgG	immunoglobulin g
IL1β	interleukin 1 beta
IL6	interleukin 6
MAPK	mitogen-activated protein kinases
NAD	nicotinamide adenine dinucleotide
NEFA	non-esterified fatty acid
NMN	nicotinamide mononucleotide
PBEF	pre-B-cell enhancing fator
PCK1	phosphoenolpyruvate carboxykinase 1
QUICKI	quanitative insulin sensitivity check index
SREBF1	sterol-regulatory element binding transcription factor 1
SVF	stromal vascular fraction
TNFα	tumour necrosis fator alpha

Introduction

Type 2 diabetes is characterized by the presence of peripheral insulin resistance and pancreatic beta-cell dysfunction [1]. Determining the precise pathophysiological mechanisms responsible for these processes is essential for development of novel therapeutics.

Serum concentrations of eNAMPT (also referred to as visfatin/PBEF) are commonly elevated in type 2 diabetes patients [2], where raised eNAMPT levels strongly correlate with declining beta-cell function [3]. This implies a pathophysiological role for eNAMPT in type 2 diabetes. However, other studies have reported insulin sensitizing and beta-cell protective effects of eNAMPT [4-7]. Therefore the precise relationship between elevated eNAMPT and type 2 diabetes remains unresolved.

Nicotinamide phosphoribosyltransferase exists in intra-cellular (iNAMPT) and extra-cellular (eNAMPT) forms. iNAMPT is widely expressed and well characterized as an NAD-biosynthetic enzyme [8]. However, the function of eNAMPT is unclear, with putative pro-inflammatory [9, 10], insulin-mimetic [11] and NAD-biosynthetic functions [5,12,13] described. These disparate reported functions are controversial and have been challenged [11, 14], but may be explained by the presence of structurally and functionally distinct monomer (50 kDa) and dimer (100 kDa) forms of eNAMPT. Dimerization is reportedly essential for NAD-biosynthetic functions [5, 15]. eNAMPT-monomer potentially exerts NAD-independent pro-inflammatory effects. However, these potential structure-function relationships have not been fully investigated, particularly within the context of type 2 diabetes pathophysiology.

Given the crucial role of chronic inflammation in type 2 diabetes pathophysiology, we hypothesize that eNAMPT-monomer will be selectively elevated in type 2 diabetes, and potentially acting in a pro-inflammatory manner, may play a key role in type 2 diabetes pathophysiology.

Methods

Animal studies For immuno-neutralization experiments, eight-week old C57Bl/6 mice (Charles River, Margate, UK) were fed high-fat (HFD; 60% w/w fat-58Y1; Test Diets, St. Louis, MO, USA) or control (CON) diets for 10 or 13 weeks and administered a rabbit polyclonal eNAMPT-antibody targeting mouse eNAMPT (2.5 μg/ml; I.P; LifespanBio, WA, USA; LS-C48964) or non-immune IgG equivalent (2 doses/week for 2 weeks) in weeks 9 – 10. Mice were either sacrificed directly post-treatment (10 weeks) or 3 weeks post-dose (13 weeks) (n=24/group)

For experimental elevation of eNAMPT and NMN, mice were administered either recombinant eNAMPT (Adipogen, Seoul, South Korea; I.P.; 5ng/ml/day), NMN (Sigma, Poole, UK; I.P.; 500 mg/kg body weight/day), or saline equivalent for 14 days (n=8/group).

Mice were maintained on a 12 h light/12 h dark cycle. Animal experiments were conducted in accordance with UK Home Office Animals (Scientific Procedures) Act 1986, with local ethical committee approval. Experimenters were not blind to group assignment and outcome assessment.

IPGTT and in vivo insulin secretion Mice were fasted overnight then administered 2 g/kg body weight 25% w/v. dextrose (I.P; Sigma). Blood glucose (tail vein) was measured (Accuchek, Roche Diagnostics, Burgess Hill, UK) between 0 – 120 min. Additional blood was collected during IPGTT to estimate insulin secretory response to glucose.

Model Assessments of Insulin resistance Whole-body insulin resistance and sensitivity were assessed using; (A) fasting glucose x fasting insulin product, (B) HOMA-IR (log HOMA-IR = log [fasting insulin × fasting glucose/22.5] and (C) QUICKI = (1/log [fasting insulin] + log [fasting glucose]).

Blood Chemistry Blood was obtained by cardiac puncture. Serum and liver triacylglycerol levels were determined by colourimetric assay kit (Cayman Chemical, Ann Arbor, MI, USA). Serum NEFA levels were measured by fluorometric assay (Abcam, Cambridge, UK). ELISA kits were used to measure serum insulin (Mercodia, Uppsala, Sweden); eNAMPT (Caltag, Buckingham, UK) and TNFα, IL1β and MCP1 (eBioscience, Hatfeild, UK).

Serum NMN and tissue NAD levels Serum NMN was detected fluorometrically by HPLC, using a modified version of a previously described methodology [16]. See electronic supplementary material (ESM) Methods. Tissue NAD levels were determined using an NAD/NADH quantitation kit (Sigma)

Immunoblotting Immunoblotting was conducted as previously described [17]. Primary antibodies against NAMPT (Sigma or Bethyl Laboratories, Montgomery, TX, USA), phospho(Ser^{473})AKT and total-AKT (both Cell Signaling Technologies, MA, USA) were used in this study (all primary antibodies were rabbit anti-mouse polyclonal and were used at 1:1000 dilutions). Immunoprecipitation of NAMPT was conducting using a Catch and Release Reversible Immunoprecipitation System (Millipore, Watford, UK).

Quantitative RT-PCR Gene expression was determined by Taqman or Sybr green qRT-PCR [17], where gene expression was measured by ΔΔCt methodology, normalised against 18S ribosomal RNA (Applied Biosystems, UK). Changes in gene expression are represented as fold change relative to one, where control equals one. For primer details (all Eurogentec, Southampton, UK) see ESM Table 1

Mouse Islet isolation and insulin secretion Mouse pancreases were digested in 2 ml Hanks Buffered Salt Solution (HBSS) containing collagenase P (1 mg/ml) and DNAse I (0.15 mg/ml; both Roche

Diagnostics). Islets were hand-picked into RPMI 1640 media for RNA extraction or insulin secretion assays. For islet insulin-secretion assays, batches of eight size-matched islets were pre-incubated for 1 h at 37ºC in HBSS containing 3 mM glucose, 10 mM HEPES (pH 7.4) and 0.2% BSA (w/v). For glucose-stimulated insulin secretion (GSIS), islets were incubated for 1 h at 37ºC in HBSS (10 mM HEPES (pH 7.4), 0.2% BSA) supplemented with 3 mM or 17 mM glucose. After 1 h media was collected for determination of insulin levels by ELISA. See ESM Methods

Immunofluorescence of Mouse Pancreatic Sections Immunostaining was conducted as previously described [7]. Briefly, whole pancreas was fixed in buffered formalin, paraffin-embedded, cut into sections and stained with either guinea-pig anti-insulin (1:100; Abcam) and/or rabbit anti-phospho-P38 (1:1600; Cell Signaling Technologies) antibody. Sections were then mounted on glass cover slips and analyzed using a Leica DM5000 Epi-Fluorescent microscope and Leica Application Suite software. See ESM Methods

MIN6 Cell culture and treatment MIN6 beta-cells were incubated with eNAMPT (2 – 10 ng/ml; Adipogen) with or without eNAMPT-Ab (2.5 μg/ml; LS-C48964) and analysed for changes in insulin secretion or NAD levels. See ESM Methods

Isolation of white adipocytes and stromal vascular fraction (SVF). White adipocytes and SVF were isolated from epidymal white AT according to previously described methodology [18]. Isolated adipocyte and SVF preparations were incubated for 3.5 h at 37°C in DMEM containing 25 mM glucose. Media was then collected and analysed for eNAMPT content by ELISA.

Statistical Analysis Results are expressed as mean ± SEM. Statistical differences were calculated by one-way ANOVA and Tukey's Post-test where appropriate (GraphPad Software, CA, USA)**.**

Results

High-fat feeding selectively induces production and secretion of eNAMPT-monomer We first demonstrated that serum eNAMPT levels were elevated in diabetic HFD mice (Fig. 1A).

We next examined whether increased total eNAMPT was associated with specific changes in eNAMPT-monomer or -dimer, using non-reducing SDS-PAGE and immunoblotting. Indicative of a selective diabetogenic function, eNAMPT-monomer protein levels were in markedly elevated in serum (82 ± 1.86%; Fig. 1B – C) of HFD mice compared to CON. In contrast, serum levels of eNAMPT-dimer and its reaction product NMN (Fig. 1B – D) were marginally reduced or unchanged between HFD and CON. Similar changes were observed in white adipose tissue (AT), a major source of circulating eNAMPT. White AT from HFD mice displayed increases in *Nampt* mRNA levels (Fig. 1E), with parallel increases in NAMPT-monomer (64 ± 5.9%) but without any observed changes in NAMPT-dimer and NAD (Fig. 1F – H). Therefore, alterations in levels and structure of NAMPT in white AT provide a potential explanation for increased serum eNAMPT-monomer and -dimer in HFD mice.

To further examine the source of eNAMPT, we isolated white adipocytes and SVF from epididymal white AT and measured eNAMPT secretion. In white adipocytes isolated from HFD mice, eNAMPT secretion was markedly decreased, whilst in SVF isolated from HFD mice eNAMPT secretion was increased (Fig. 1I – J). Collectively, this suggests that white adipocytes and SVF are likely the primary source of eNAMPT-dimer and –monomer, respectively. The cellular source of eNAMPT-monomer within the SVF requires further study, however previous studies have reported eNAMPT secretion from undifferentiated pre-adipocytes and immune cells including macrophages, neutrophils and B-cells.

Together these data demonstrate that serum levels of eNAMPT-monomer are selectively elevated in diabetic HFD mice. This implies a specific pathophysiological role for eNAMPT-monomer in experimental diabetes.

eNAMPT-Ab improves glycemic control and insulin resistance in HFD mice. To determine the importance of raised serum eNAMPT-monomer levels in experimental diabetes, CON and HFD fed mice were administered eNAMPT antibody (eNAMPT-Ab; 2 doses/week in weeks 9 – 10) or non-immune IgG equivalent. Immuno-neutralization allows for selective inhibition of circulating eNAMPT, without inhibiting iNAMPT. Immunoprecipitation of NAMPT with this antibody followed by immunoblot led to detection of band at 50 kDa but not 100 kDa (ESM Fig. 1A – B), indicating antibody specificity for eNAMPT-monomer. Moreover, eNAMPT-Ab blocked NAD-independent eNAMPT-mediated decreases in glucose-stimulated insulin secretion (GSIS) in MIN6 cells but did not have any effect on levels of NMN (the eNAMPT-dimer reaction product) in CON or HFD mice. (ESM Fig. 1C – D). This implies that the eNAMPT-Ab used here selectively targets eNAMPT-monomer. Serum levels of total-eNAMPT were non-significantly reduced following eNAMPT-Ab treatment (ESM Fig. 1E).

In support of a diabetogenic role of eNAMPT-monomer, eNAMPT-Ab administration reduced blood glucose and insulin levels (Fig. 2A – C) and corrected impaired glucose tolerance (IGT) (Fig. 2D – F) in HFD mice. As determined by assessment of insulin x glucose product, HOMA-IR and QUICKI, eNAMPT-Ab also ameliorated whole-body insulin resistance (Fig. 2G – 2I). Improved glucose tolerance and insulin sensitivity was associated with reduced fasting serum triacylglycerol and fed serum NEFA levels, although the latter did not reach significance. Fed serum triacylglycerol levels were unchanged across all groups (ESM 2A – C). Body weight and food intake were also unchanged (ESM 2D – E).

Together these data demonstrate that neutralising eNAMPT-monomer leads to a marked improvement in diabetic phenotype in HFD mice.

eNAMPT-Ab improves pancreatic islet function and increases islet size in HFD mice. Type 2 diabetes is characterized by progressive pancreatic beta-cell failure [1]. Therefore, we assessed whether

eNAMPT-Ab mediated improvements in glycemic control were mediated by improvements in beta-cell/islet health.

Beta-cell/islet function was impaired in HFD mice, as evidenced by a lack of islet compensatory response to insulin resistance in static *ex vivo* GSIS studies (Fig. 3A) and *in vivo* measurements of 1st (0 – 15 minutes) and 2nd phase (15 – 60 minutes) insulin secretory response to glucose (Fig. 3B – C). Crucially, eNAMPT immuno-neutralisation restored islet compensation, demonstrated by a marked increase in *ex vivo* GSIS and *in vivo* 1st phase insulin secretion in HFD^{Ab} mice.

We next assessed the effects of eNAMPT-Ab on islet size. Islet size was reduced by 46% ($P<0.01$) in HFD^{IgG} mice compared to CON^{IgG}, an effect that was completely reversed by eNAMPT-Ab (Fig. 3D – E). Several studies have observed increased islet size in HFD mice. However, the reduced islet size observed here likely reflect progression from insulin resistance to an overt diabetic phenotype in our model. Beta-cell apoptosis and necrosis are commonly attributed mechanisms for reduced beta-cell/islet mass in type 2 diabetes. Consistent with this, islet mRNA levels of pro-apoptotic and necrotic markers were significantly elevated in HFD mice (Fig. 3F). Strikingly, mRNA levels of these genes were lowered to basal levels following eNAMPT-Ab administration, demonstrating that eNAMPT immuno-neutralisation improves beta-cell function/mass in part by protecting against beta-cell apoptosis and necrosis. Together these data demonstrate that eNAMPT immuno-neutralisation improves glycemic control in HFD mice in part through reversing beta-cell dysfunction and restoring islet compensation.

eNAMPT-Ab improves hepatic insulin sensitivity and reduces hepatic fat content. Obesity-induced non-alcoholic fatty liver disease (NAFLD), characterized by excess hepatic lipid accumulation and inflammation, is an established risk factor for development of hepatic insulin resistance and type 2 diabetes [19]. Elevated serum eNAMPT levels in NAFLD are associated with worsening disease severity [20]. Consistent with a potential role for eNAMPT-monomer in development of fatty liver, eNAMPT-Ab reversed HFD-mediated increases in hepatic triacylglycerol content (ESM Fig. 3A) and

Srebf1 and *Fasn* lipogenic gene expression (ESM Fig. 3B). Hepatic insulin resistance is strongly associated with increased liver lipid content. Moreover, eNAMPT-Ab reversed HFD-mediated decreases in hepatic protein levels of phosphorylated-(Ser^{473})-AKT, a marker of insulin signalling (ESM Fig. 3C), and corrected abnormally elevated mRNA levels of *Pck1* (ESM Fig. 3B), a key gluconeogenic gene. Together, these data suggest that eNAMPT immuno-neutralisation lowers hepatic lipid content and may improve hepatic insulin sensitivity in HFD mice.

eNAMPT-Ab ameliorates tissue and systemic inflammation in HFD mice. Chronic inflammation is causal for beta-cell failure in type 2 diabetes [21]. Pro-inflammatory functions of eNAMPT are reported, although such studies have not distinguished between monomer and dimer [10], or examined a specific pro-inflammatory role of eNAMPT in type 2 diabetes. eNAMPT-Ab lowered HFD-mediated increases in serum Ccl2 (MCP1) levels (Fig. 4A), although serum TNFα and IL1β were unchanged across all groups (Fig. 4B – C). Furthermore, eNAMPT-Ab reversed HFD-mediated increases in islet mRNA levels of pro-inflammatory cytokines (*Tnfa*, *Il1b*, *Il6*) chemokines (*Ccl2*) and immune cell markers: *Itgam* (Cd11b), *Itgax* (Cd11c)*, Adgre1* (F4/80) (Fig. 4D). Studies in monocytes have reported that eNAMPT induces pro-inflammatory cytokine production in part through activation of p-38 MAPK [10]. In agreement, we show that islet phospho-p38 immunofluorescence signal (denoting activated p38) was enhanced in HFD mice compared to CON, an effect that was reversed by eNAMPT-Ab (Fig. 4E). Chronic inflammation in liver and white AT is also common in obesity and type 2 diabetes and plays a crucial role in disease pathophysiology. Consistent with a pro-inflammatory effect of eNAMPT-monomer in these tissues, eNAMPT-Ab lowered expression of pro-inflammatory genes in liver and AT of HFD mice (Fig. 4F – G). These data provide strong support for the notion that eNAMPT immuno-neutralisation improves pancreatic beta-cell health and peripheral insulin resistance through resolution of inflammation in HFD-mice, and that eNAMPT-monomer likely exerts pro-inflammatory effects.

The beneficial effects of eNAMPT-Ab are maintained three weeks post-dose. To determine whether the effects of eNAMPT immuno-neutralisation were maintained over time, eNAMPT-Ab was administered in weeks 9 – 10 as previously. Mice then remained on CON or HFD diets until week 13 without further eNAMPT-Ab administration. At three-weeks post-dose, eNAMPT-Ab lowered HFD-mediated increases in blood glucose enhanced islet insulin secretion, reduced islet inflammation and reduced hepatic triacylglycerol content, hepatic lipogenic gene expression and hepatic inflammation (Fig. 5A – F). Thus, the beneficial effects of one dose regimen of eNAMPT-Ab are maintained at least a three weeks post treatment.

14-day eNAMPT monomer administration induces a diabetic phenotype in mice. Finally, we examined the impact of experimental elevation of serum eNAMPT-monomer on glycaemic control in mice. Lean, non-diabetic mice were administered recombinant eNAMPT or saline equivalent. eNAMPT administration doubled serum eNAMPT levels to 3.05 ± 0.37 ng/ml (Fig 6A), similar to concentrations in HFD mice. When recombinant eNAMPT protein was analysed using non-reducing SDS-PAGE and immunoblotting, a band was detected at 50 kDa but not 100 kDa (ESM Fig. 1E). Moreover, recombinant eNAMPT treatment did not increase NAD levels *in vitro* in MIN6 cells nor *in vivo* in mouse white AT (ESM Fig. 1G – H). This suggests that the recombinant eNAMPT used in this study does not dimerize and promote NAD biosynthesis and thus represents eNAMPT-monomer. Therefore, to mimic elevated eNAMPT-dimer, a separate group of mice were administered NMN, the reaction product of the eNAMPT-dimer NAD biosynthetic reaction.

14-day eNAMPT-monomer administration resulted in elevated fasting blood glucose levels (Fig. 6B), development of IGT (0 – 30 minutes post-glucose injection) (Fig 6C) and whole-body insulin resistance, determined by HOMA-IR and QUICKI (Fig. 6D –E). These changes were not related to changes in body weight, serum triacylglycerol or insulin levels (ESM Fig. 4A – D). Moreover, eNAMPT-monomer administration led to impaired insulin secretion, demonstrated by a lack of islet compensatory response to insulin resistance (Fig. 6F –G). Consistent with hypothesized pro-

inflammatory actions, eNAMPT-monomer administration led to elevated serum levels of MCP1 (Fig. 6H) and increased liver and white AT *Ccl2* mRNA (Fig. 6I), although serum IL1β and TNFα and liver and white AT mRNA levels of a number of other pro-inflammatory markers remained unchanged (ESM Fig. 4E – H). eNAMPT-monomer administration induced a non-significant trend towards increased pro-inflammatory gene expression in islets (ESM Fig. 4I).

In contrast to the diabetogenic effects of eNAMPT-monomer, NMN administration resulted in mild reductions in blood glucose and serum IL1β, without changes in body weight, glucose tolerance, and insulin sensitivity (ESM Fig. 5).

Together these data suggest distinct structure-function characteristics of eNAMPT-monomer and -dimer; eNAMPT-monomer induces a diabetic phenotype in mice, via NAD-independent pro-inflammatory effects, whilst eNAMPT-dimer/NMN elevation led to mild improvements in glycemic control.

Discussion

We provide multiple lines of evidence suggesting an important role for NAD-independent eNAMPT-monomer in type 2 diabetes; (1) Diabetic HFD mice display a selective increase in serum eNAMPT-monomer; (2) Blocking eNAMPT action reversed the diabetogenic effects of HFD; (3) 14-day administration of NAD-independent eNAMPT-monomer induced a diabetic phenotype in non-diabetic mice.

Elevated serum eNAMPT levels are reported in type 2 diabetes [2, 3, 20, 22-24], although contrasting studies have observed decreased or unchanged serum eNAMPT in metabolic diseases [25, 26]. However, these studies have not specifically examined eNAMPT function or distinguished between eNAMPT monomer or dimer.

Our findings go some way to clarifying contradictory findings regarding eNAMPT and type 2 diabetes by demonstrating differences between levels of eNAMPT-monomer and -dimer in experimental

diabetes and highlighting the relevance of structure-function differences between monomer and dimer.

The precise function of eNAMPT and the relationship between raised eNAMPT levels and type 2 diabetes pathophysiology remain unresolved. Previous experimental studies have demonstrated both beneficial and deleterious effects of recombinant eNAMPT on insulin secretion and sensitivity *in vitro* [27-30]. However these studies have often examined acute effects of eNAMPT, which is unlikely to accurately represent a diabetic phenotype, or have used supraphysiological concentrations of eNAMPT. Crucially, these studies also did not distinguish between eNAMPT-monomer and -dimer.

Our studies, and those of other groups, have described beneficial acute and chronic effects of NMN, the reaction product of the eNAMPT-dimer biosynthetic reaction [4, 6, 7, 31, 32]. Consistent with a beneficial effect of eNAMPT-dimer, serum and white AT eNAMPT-dimer were unchanged or decreased in HFD mice, whilst 14-day NMN administration lowered blood glucose and inflammation in non-diabetic mice. In contrast, we describe a specific role for eNAMPT-monomer in experimental diabetes, functioning in part through NAD-independent pro-inflammatory effects. Pro-inflammatory effects of eNAMPT in type 2 diabetes have not previously been reported. However, our findings are broadly in agreement with studies of eNAMPT in other diseases, although such studies did not distinguish between monomer and dimer. For example, eNAMPT has been reported to induce monocyte expression and secretion of IL6, IL1β and TNFα [10], potentially via receptor-mediated mechanisms [33]. Thus, normalisation of eNAMPT-monomer signaling in type 2 diabetes would be predicted to resolve inflammation-mediated beta-cell dysfunction and insulin resistance and improve glycaemic control.

We hypothesise that increased monomer levels are in part related to AT dysfunction. AT-derived eNAMPT-dimer is secreted from fully differentiated adipocytes, whilst monomer may be secreted from poorly-differentiated adipocytes and immune cells [5, 9, 10, 34-36]. Since poor adipocyte

differentiation and immune cell infiltration are characteristics of obese AT [37], we hypothesise that such pathophysiological changes could explain increased monomer levels in HFD mice. In agreement, in HFD mice eNAMPT secretion from the AT SVF, which contains immune cells and undifferentiated pre-adipocytes, was markedly increased. Thus we hypothesise obesity-mediated AT dysfunction results in a phenotypic switch, characterised by elevated eNAMPT-monomer production from SVF and reduced dimer secretion from adipocytes. Future studies will elucidate the precise mechanisms involved in dimer formation and identify the main cellular source of eNAMPT within the SVF.

Together, these studies suggest that eNAMPT-monomer is an attractive therapeutic target for treatment of type 2 diabetes. Future strategies to develop this therapeutic approach will include development of eNAMPT-monomer receptor antagonists, specific eNAMPT-monomer inhibitors and humanized eNAMPT monoclonal antibodies (mAbs). Humanized mAbs can be engineered with an extended half-life, potentially allowing clinical benefits to be achieved with only one dose every 1 – 3 months [38], providing benefits in terms of cost, convenience and compliance.

In summary, we demonstrate that elevated eNAMPT-monomer contributes to development of type 2 diabetes pathophysiology. In addition, we provide proof-of-concept evidence that selectively blocking the action of eNAMPT-monomer represents a promising therapeutic strategy for treatment of type 2 diabetes.

Funding

This work was supported by the following funding: European Foundation for the Study of Diabetes/Lilly fellowship, Society for Endocrinology Early Career Grant and Diabetes UK project grant (15/0005154) (all PWC). MFS was funded by FUNDACAO PARA A CIENCIA E TECNOLOGIA, Ministerio da Educacao e Ciencia, Portugal. JK, SMH and MMY are supported by the Bart's and the London National Institute of Health Research Cardiovascular Biomedical Research Unit.

The authors declare that there is no duality interest associated with this manuscript.

Author Contributions

PWC is responsible for the integrity of the work as a whole. JK, SRS, MFS, SMH, MMY and PWC designed research, analysed data and reviewed and approved the final manuscript; JK, SRS, MFS, SMH and PWC performed research; PWC wrote the paper.

Acknowledgements

Some of the data in this manuscript were presented in abstract form at the American Diabetes Association Scientific Sessions meeting in 2015 and at the Diabetes UK professional conference meeting in 2016

References

[1] DeFronzo RA, Abdul-Ghani MA (2011) Preservation of beta-cell function: the key to diabetes prevention. The Journal of clinical endocrinology and metabolism 96: 2354-2366

[2] Chang YH, Chang DM, Lin KC, Shin SJ, Lee YJ (2011) Visfatin in overweight/obesity, type 2 diabetes mellitus, insulin resistance, metabolic syndrome and cardiovascular diseases: a meta-analysis and systemic review. Diabetes/metabolism research and reviews 27: 515-527

[3] Lopez-Bermejo A, Chico-Julia B, Fernandez-Balsells M, et al. (2006) Serum visfatin increases with progressive beta-cell deterioration. Diabetes 55: 2871-2875

[4] Yoshino J, Mills KF, Yoon MJ, Imai S (2011) Nicotinamide mononucleotide, a key NAD(+) intermediate, treats the pathophysiology of diet- and age-induced diabetes in mice. Cell metabolism 14: 528-536

[5] Revollo JR, Korner A, Mills KF, et al. (2007) Nampt/PBEF/Visfatin regulates insulin secretion in beta cells as a systemic NAD biosynthetic enzyme. Cell metabolism 6: 363-375

[6] Caton PW, Kieswich J, Yaqoob MM, Holness MJ, Sugden MC (2011) Nicotinamide mononucleotide protects against pro-inflammatory cytokine-mediated impairment of mouse islet function. Diabetologia 54: 3083-3092

[7] Caton PW, Richardson SJ, Kieswich J, et al. (2013) Sirtuin 3 regulates mouse pancreatic beta cell function and is suppressed in pancreatic islets isolated from human type 2 diabetic patients. Diabetologia 56: 1068-1077

[8] Imai S (2009) Nicotinamide phosphoribosyltransferase (Nampt): a link between NAD biology, metabolism, and diseases. Current pharmaceutical design 15: 20-28

[9] Samal B, Sun Y, Stearns G, Xie C, Suggs S, McNiece I (1994) Cloning and characterization of the cDNA encoding a novel human pre-B-cell colony-enhancing factor. Molecular and cellular biology 14: 1431-1437

[10] Moschen AR, Kaser A, Enrich B, et al. (2007) Visfatin, an adipocytokine with proinflammatory and immunomodulating properties. Journal of immunology 178: 1748-1758

[11] Fukuhara A, Matsuda M, Nishizawa M, et al. (2005) Visfatin: a protein secreted by visceral fat that mimics the effects of insulin. Science 307: 426-430

[12] Rongvaux A, Shea RJ, Mulks MH, et al. (2002) Pre-B-cell colony-enhancing factor, whose expression is up-regulated in activated lymphocytes, is a nicotinamide phosphoribosyltransferase, a cytosolic enzyme involved in NAD biosynthesis. European journal of immunology 32: 3225-3234

[13] Yoon MJ, Yoshida M, Johnson S, et al. (2015) SIRT1-Mediated eNAMPT Secretion from Adipose Tissue Regulates Hypothalamic NAD and Function in Mice. Cell metabolism

[14] Hara N, Yamada K, Shibata T, Osago H, Tsuchiya M (2011) Nicotinamide phosphoribosyltransferase/visfatin does not catalyze nicotinamide mononucleotide formation in blood plasma. PloS one 6: e22781

[15] Wang T, Zhang X, Bheda P, Revollo JR, Imai S, Wolberger C (2006) Structure of Nampt/PBEF/visfatin, a mammalian NAD+ biosynthetic enzyme. Nature structural & molecular biology 13: 661-662

[16] Formentini L, Moroni F, Chiarugi A (2009) Detection and pharmacological modulation of nicotinamide mononucleotide (NMN) in vitro and in vivo. Biochemical pharmacology 77: 1612-1620

[17] Caton PW, Nayuni NK, Kieswich J, Khan NQ, Yaqoob MM, Corder R (2010) Metformin suppresses hepatic gluconeogenesis through induction of SIRT1 and GCN5. The Journal of endocrinology 205: 97-106

[18] Weisberg SP, McCann D, Desai M, Rosenbaum M, Leibel RL, Ferrante AW, Jr. (2003) Obesity is associated with macrophage accumulation in adipose tissue. The Journal of clinical investigation 112: 1796-1808

[19] Birkenfeld AL, Shulman GI (2014) Nonalcoholic fatty liver disease, hepatic insulin resistance, and type 2 diabetes. Hepatology 59: 713-723
[20] Moschen AR, Gerner RR, Tilg H (2010) Pre-B cell colony enhancing factor/NAMPT/visfatin in inflammation and obesity-related disorders. Current pharmaceutical design 16: 1913-1920
[21] Donath MY, Shoelson SE (2011) Type 2 diabetes as an inflammatory disease. Nature reviews Immunology 11: 98-107
[22] Chen MP, Chung FM, Chang DM, et al. (2006) Elevated plasma level of visfatin/pre-B cell colony-enhancing factor in patients with type 2 diabetes mellitus. The Journal of clinical endocrinology and metabolism 91: 295-299
[23] Haider DG, Holzer G, Schaller G, et al. (2006) The adipokine visfatin is markedly elevated in obese children. Journal of pediatric gastroenterology and nutrition 43: 548-549
[24] Krzyzanowska K, Krugluger W, Mittermayer F, et al. (2006) Increased visfatin concentrations in women with gestational diabetes mellitus. Clinical science 110: 605-609
[25] Pagano C, Pilon C, Olivieri M, et al. (2006) Reduced plasma visfatin/pre-B cell colony-enhancing factor in obesity is not related to insulin resistance in humans. The Journal of clinical endocrinology and metabolism 91: 3165-3170
[26] Berndt J, Kloting N, Kralisch S, et al. (2005) Plasma visfatin concentrations and fat depot-specific mRNA expression in humans. Diabetes 54: 2911-2916
[27] Kim da S, Kang S, Moon NR, Park S (2014) Central visfatin potentiates glucose-stimulated insulin secretion and beta-cell mass without increasing serum visfatin levels in diabetic rats. Cytokine 65: 159-166
[28] Cheng Q, Dong W, Qian L, Wu J, Peng Y (2011) Visfatin inhibits apoptosis of pancreatic beta-cell line, MIN6, via the mitogen-activated protein kinase/phosphoinositide 3-kinase pathway. Journal of molecular endocrinology 47: 13-21
[29] Brown JE, Onyango DJ, Ramanjaneya M, et al. (2010) Visfatin regulates insulin secretion, insulin receptor signalling and mRNA expression of diabetes-related genes in mouse pancreatic beta-cells. Journal of molecular endocrinology 44: 171-178
[30] Oita RC, Ferdinando D, Wilson S, Bunce C, Mazzatti DJ (2010) Visfatin induces oxidative stress in differentiated C2C12 myotubes in an Akt- and MAPK-independent, NFkB-dependent manner. Pflugers Archiv : European journal of physiology 459: 619-630
[31] Ramsey KM, Mills KF, Satoh A, Imai S (2008) Age-associated loss of Sirt1-mediated enhancement of glucose-stimulated insulin secretion in beta cell-specific Sirt1-overexpressing (BESTO) mice. Aging cell 7: 78-88
[32] Spinnler R, Gorski T, Stolz K, et al. (2013) The adipocytokine Nampt and its product NMN have no effect on beta-cell survival but potentiate glucose stimulated insulin secretion. PloS one 8: e54106
[33] Camp SM, Ceco E, Evenoski CL *et al*. (2015) Unique Toll-Like Receptor 4 Activation by NAMPT/PBEF Induces NFκB Signaling and Inflammatory Lung Injury. Science Reports 14;5:13135
[34] Friebe D, Neef M, Kratzsch J, et al. (2011) Leucocytes are a major source of circulating nicotinamide phosphoribosyltransferase (NAMPT)/pre-B cell colony (PBEF)/visfatin linking obesity and inflammation in humans. Diabetologia 54: 1200-1211
[35] Dahl TB, Yndestad A, Skjelland M, et al. (2007) Increased expression of visfatin in macrophages of human unstable carotid and coronary atherosclerosis: possible role in inflammation and plaque destabilization. Circulation 115: 972-980
[36] Curat CA, Wegner V, Sengenes C, et al. (2006) Macrophages in human visceral adipose tissue: increased accumulation in obesity and a source of resistin and visfatin. Diabetologia 49: 744-747
[37] Sun K, Kusminski CM, Scherer PE (2011) Adipose tissue remodeling and obesity. The Journal of clinical investigation 121: 2094-2101

[38] Boni-Schnetzler M, Donath MY (2013) How biologics targeting the IL-1 system are being considered for the treatment of type 2 diabetes. British journal of clinical pharmacology 76: 263-268

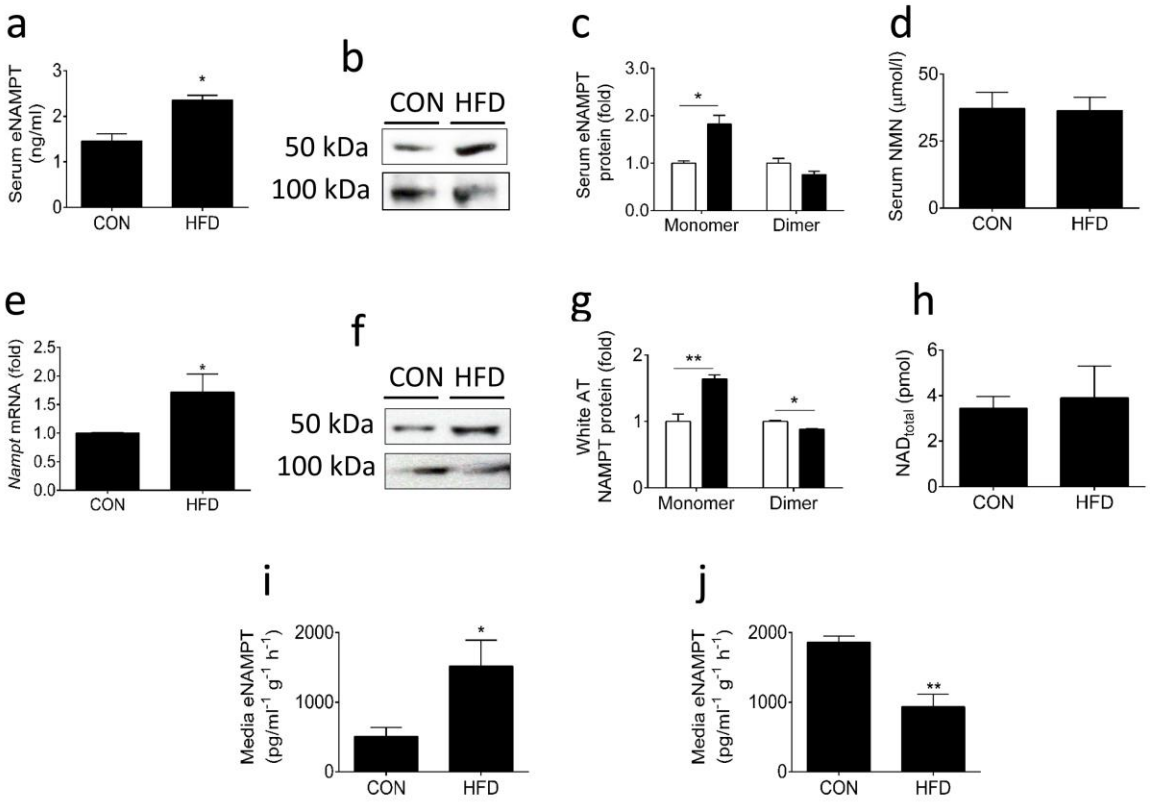

Fig. 1 eNAMPT-monomer levels are selectively elevated in HFD mice. Mice were fed CON or HFD for 10 weeks; (a) Total serum eNAMPT, (b – c) Serum eNAMPT-monomer and -dimer protein (CON=white bars; HFD = black bars), (d) Serum NMN. White AT levels of; (e) *Nampt* mRNA (f – g) NAMPT-monomer and -dimer protein (CON=white bars; HFD = black bars), (h) NAD levels. eNAMPT secretion from (i) stromal vascular fraction (SVF) and (j) white adipocytes. Western blots are representative of 3 separate blots. Statistically significant differences between groups are indicated by *p<0.05, **p<0.01.

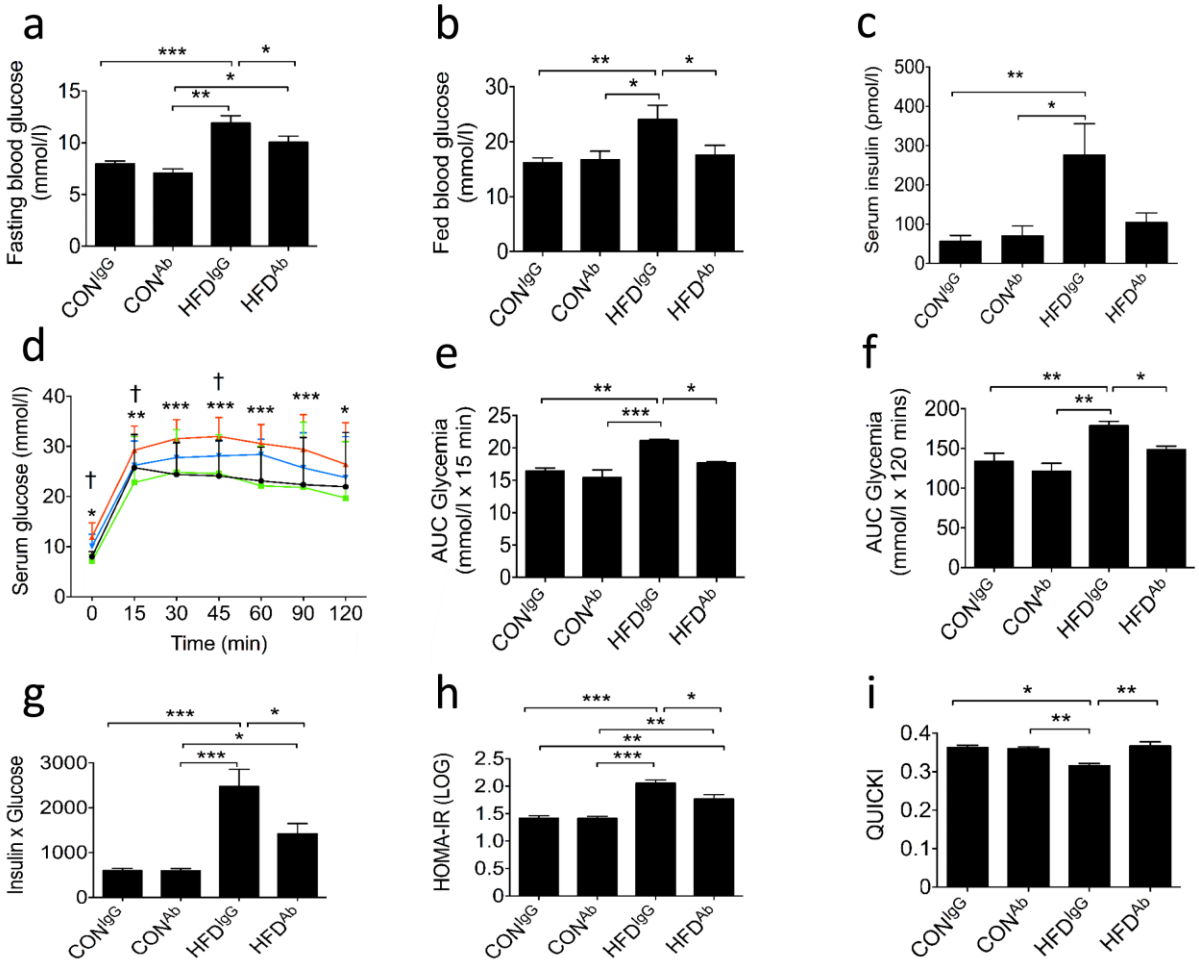

Fig. 2. eNAMPT-monomer immuno-neutralisation reverses a diabetic phenotype in HFD mice. CON and HFD mice (10 weeks) were administered eNAMPT-Ab or non-immune IgG; (a) Fed serum glucose, (b) Fasting serum glucose, (c) Fed Serum insulin, (d – f) Glucose response to IPGTT (black = CON^{IgG}, green = CON^{Ab}, red = HFD^{IgG}, blue = HFD^{Ab}). (g) Insulin x Glucose product, (h) HOMA-IR, (i) QUICKI. Statistically significant differences between groups are indicated by *p<0.05, **p<0.01, ***p<0.001, except panels f and l where differences are indicated by *p<0.05 (CON^{IgG} vs. HFD^{IgG}); †p<0.05 (HFD^{IgG} vs. HFD^{Ab}).

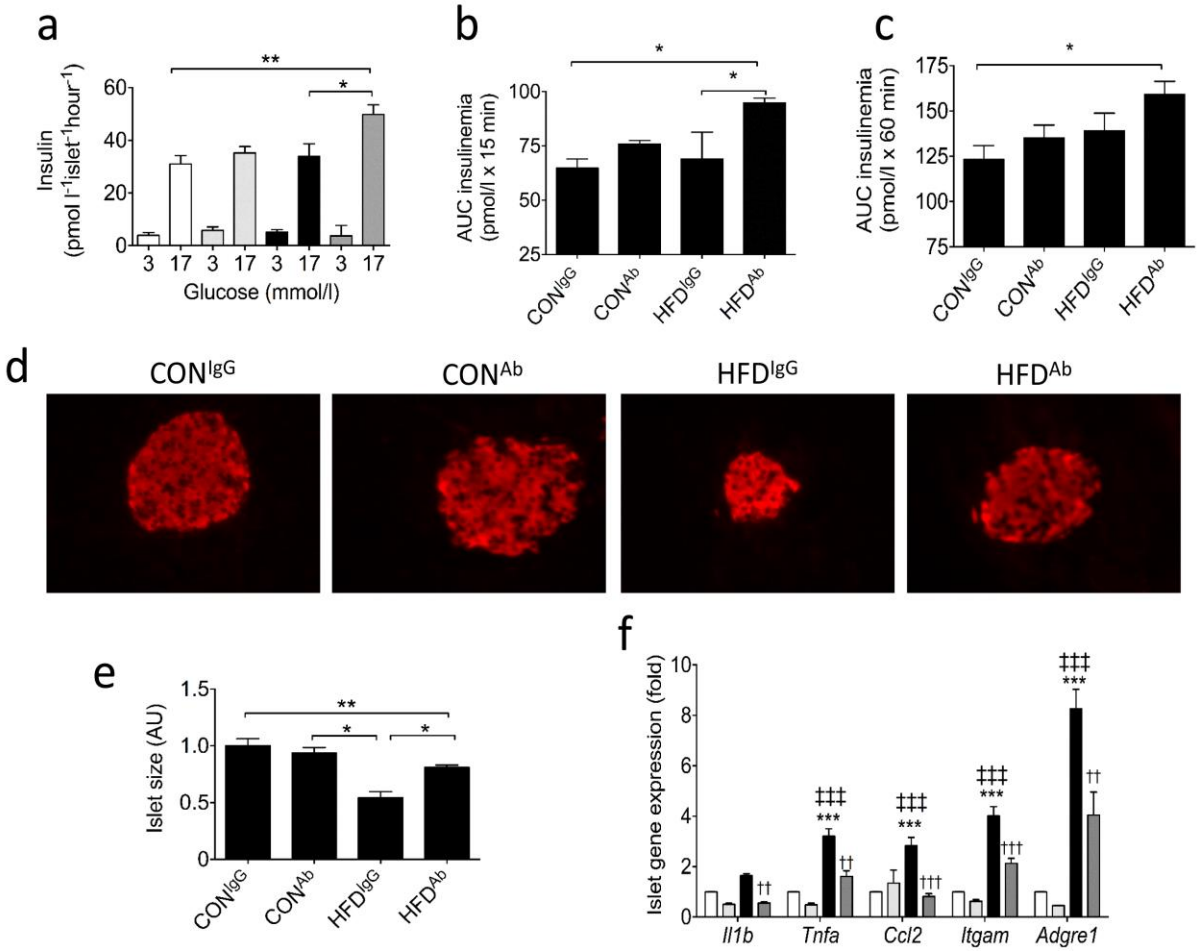

Fig. 3. eNAMPT immuno-neutralization reverses beta-cell dysfunction in HFD mice. CON and HFD mice (10 weeks) were administered eNAMPT-Ab or non-immune IgG; (a) *Ex vivo* GSIS, (b – c) AUC insulin response to IPGTT. (d) Insulin immunofluorescence staining of whole pancreatic sections (Magnification x20); (e) Relative islet size (AU); (f) Gene expression of pro-apoptotic genes in isolated islets (panels a and f: white = CON^{IgG}, light grey = CON^{Ab}, black = HFD^{IgG}, dark grey = HFD^{Ab}). Statistically significant differences between groups are indicated by *p<0.05; ** p<0.01, ***p<0.001, except panel f where differences are indicated by *p<0.05, ***p<0.001 (CON^{IgG} vs. HFD^{IgG}); by †††p<0.001 (HFD^{IgG} vs. HFD^{Ab}) and by ‡‡p<0.01, (CON^{Ab} vs. HFD^{IgG}).

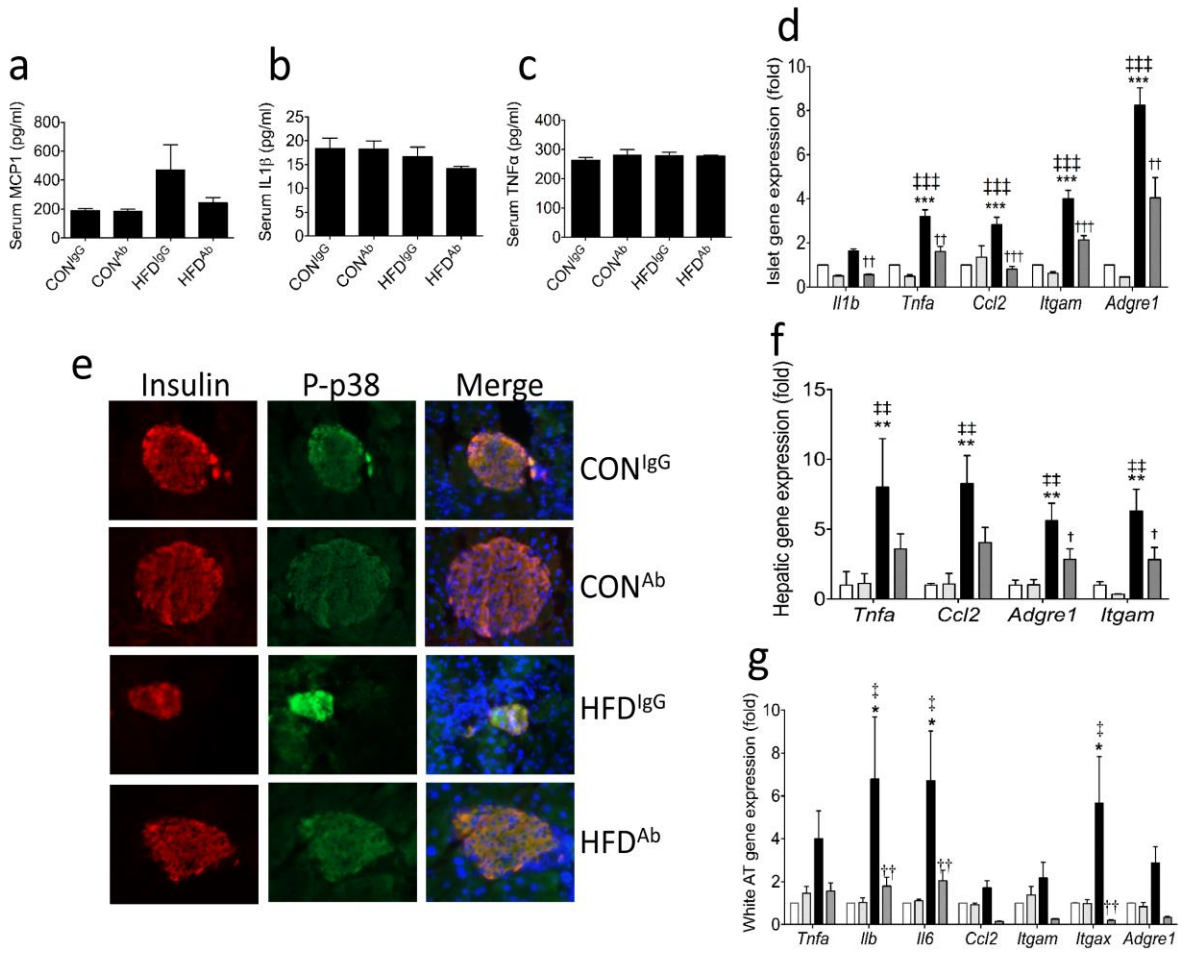

Fig. 4. eNAMPT-monomer immuno-neutralization improves tissue and systemic inflammation in HFD mice. CON and HFD mice (10 weeks) were administered eNAMPT-Ab or non-immune IgG; Serum concentrations of (a) MCP1, (b) IL1β and (c) TNFα; (d) Gene expression of pro-inflammatory genes in isolated islets; (e) Insulin and phospho-p38 islet immunofluorescence staining of whole pancreatic sections (Magnification x20); (f) Liver gene expression of pro-inflammatory genes; (g) White adipose pro-inflammatory gene expression (panels e – f : white = CON^{IgG}, light grey = CON^{Ab}, black = HFD^{IgG}, dark grey = HFD^{Ab}). Statistically significant differences are indicated by *p<0.05, **p<0.01 and ***p<0.001 (CON^{IgG} vs. HFD^{IgG}); by †p<0.05, ††p<0.01 and †††p<0.001 (HFD^{IgG} vs. HFD^{Ab}) and by ‡p<0.05, ‡‡p<0.01, ‡‡‡p<0.001 (CON^{Ab} vs. HFD^{IgG}).

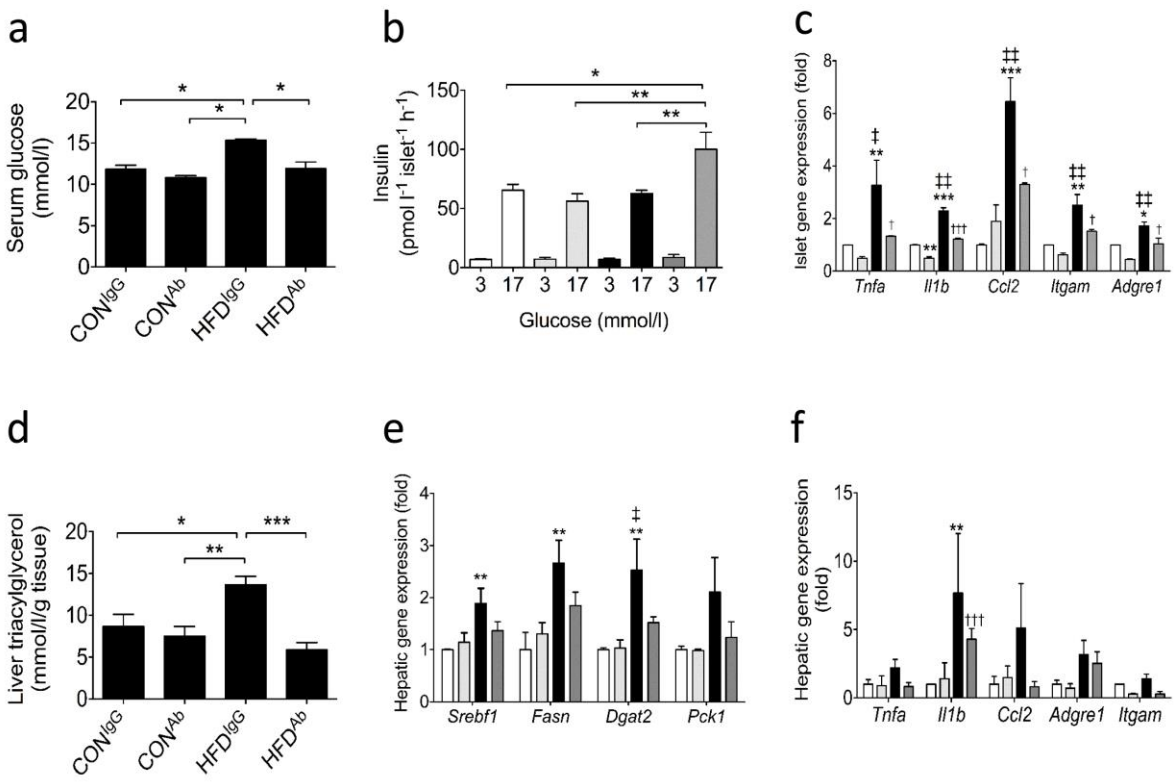

Fig. 5. The beneficial effects of eNAMPT-monomer immuno-neutralization in HFD mice are maintained three-weeks post-treatment. CON and HFD mice (13 weeks) were administered eNAMPT-Ab or non-immune IgG (weeks 9 – 10)**.** (a) Fed blood glucose, (b) *Ex vivo* GSIS, (c) Islet expression of pro-inflammatory genes, (d) Hepatic triacylglycerol levels, (e) Hepatic gene expression of lipogenic and gluconeogenic genes; (f) Liver expression of pro-inflammatory genes (panels b,c,e,f: white = CON^{IgG}, light grey = CON^{Ab}, black = HFD^{IgG}, dark grey = HFD^{Ab}). Panels a, b, d: statistically significant differences between groups are indicated by *p<0.05; **p<0.01, ***p<0.001. Panels c, e, f: statistically significant differences are indicated by *p<0.05 and ***p<0.001 (CON^{IgG} vs. HFD^{IgG}); by †p<0.05, ††p<0.01 and †††p<0.001 (HFD^{IgG} vs. HFD^{Ab}) and by ‡p<0.05, ‡‡p<0.01 (CON^{Ab} vs. HFD^{IgG}).

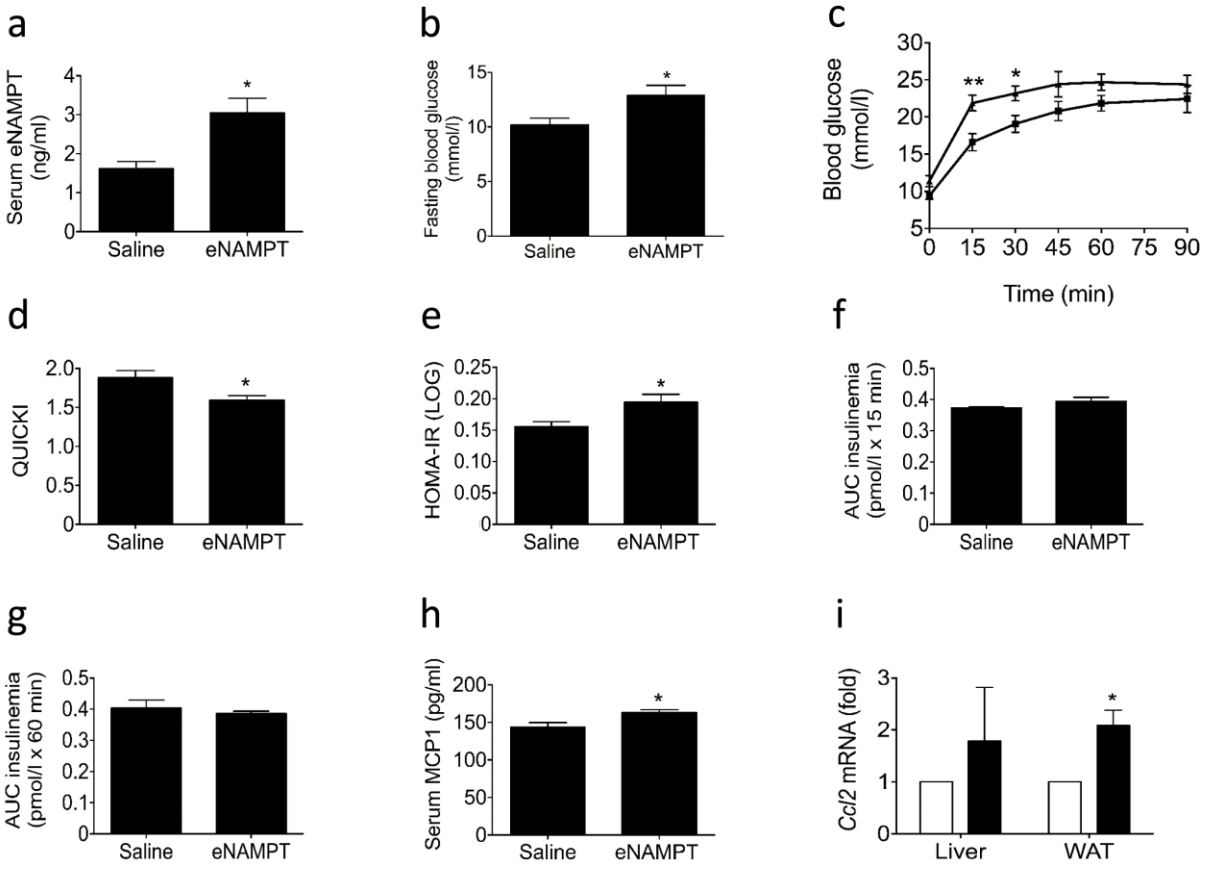

Fig. 6. 14-day eNAMPT-monomer administration induces a diabetic phenotype in mice

Mice were administered recombinant eNAMPT-monomer or saline equivalent. (a) Serum eNAMPT, (b) blood glucose, (c) IPGTT (▪ saline, ▲eNAMPT), (d) QUCKI, (e) HOMA-IR. AUC insulin response to IPGTT (f) 0 – 15 min and (g) 15 – 60 minutes, (h) Serum MCP1 levels, (i) MCP1 gene expression (white bars = saline, black bars = eNAMPT). Statistically significant differences between groups are indicated by *p<0.05, **p<0.01, ***p<0.001.

ESM Materials and Methods

Serum NMN measurements

NMN was detected fluorometrically in serum using high-performance liquid chromatography (HPLC), using a modified version of a previously described methodology (37). Plasma samples (30 μl) were extracted with 100 μl perchloric acid (1 mol/L) and then neutralized by addition of 330 μl K_2CO_3 (3 mol/L) followed by incubation at 4ºC for 10 min. Serum samples and standard solutions of NMN (30 μl; 25 – 200 μM) were subsequently derivatised by addition of 100 μl KOH (1 mol/L) and 50 μl acetophenone (Sigma, Poole, UK) followed by incubation at 4ºC for 15 min. Formic acid (100 μl) was then added and the solution incubated for 5 min at 100ºC, producing a highly fluorescent compound. Samples or standards were injected into the HPLC system consisting in a mobile phase of 0.1 M ammonium acetate and 1 mM EDTA buffer pH 5.65, 15% acetonitrile, a C18 column (15 cm length; 2 mm internal diameter) and a fluorometric detector (FP-920 Intelligent Fluorescence Detector; JASCO, Essex, UK) with excitation and emission wavelength of 332 and 454 nm, respectively.

Islet isolation

Islet isolation was conducted as previously described (6). Mouse pancreases were digested in 2 ml Hanks Buffered Salt Solution (HBSS) containing collagenase P (1 mg/ml) and DNAse I (0.15 mg/ml; both Roche Diagnostics, Burgess Hill, UK). Islets were hand-picked into RPMI 1640 media (containing 11 mol/L glucose, supplemented with 10% (v/v) heat-inactivated FBS; 100 U/ml penicillin and 100 μg/ml streptomycin; all Sigma Aldrich, Poole, UK). Isolated islets were either picked into RPMI and immediately lysed for RNA extraction or transferred to RPMI and allowed to recover for 2 h, prior to *ex vivo* insulin secretion assay.

Insulin Secretion *ex vivo*

Islet insulin-secretion assays were conducted as previously described (6). Briefly, batches of ten size-matched islets were pre-incubated for 1 h at 37ºC in HBSS containing 3 mM glucose, 10 mM HEPES (pH 7.4) and 0.2% BSA (w/v). For glucose-stimulated insulin secretion, islets were incubated for 1 h at 37ºC in HBSS (10 mol/L HEPES (pH 7.4), 0.2% w/v BSA) supplemented with 3 mol/L or 17 mol/L glucose. After 1 h media was collected and insulin levels were determined using a specific ELISA (Mercodia, Uppsala, Sweden)

Immunofluorescence of Mouse Pancreatic Sections

Islet immunostaining (27) for insulin and phospho-p38 was performed on pancreas sections that had been fixed in buffered paraformaldehyde (3.8%) and paraffin-embedded. Sections were incubated overnight at 4˚C in guinea-pig anti-insulin antibody (1:100; Abcam, Cambridge, UK) and/or rabbit anti-phospho p38 (Thr^{180}/Tyr^{182}; Cell Signaling Technologies, MA, USA) antibody (1:1600) and detected with goat anti-guinea pig AlexaFluor® 647 (1:1000) and goat anti-rabbit AlexaFluor® 488 (1:1000) conjugated secondary antibody (Invitrogen, Waltham, MA, USA), respectively. DAPI (1:1000, Invitrogen, Waltham, MA, USA) was included in the final incubation step to stain cell nuclei. Sections were mounted in Vectashield hard-set mounting medium (Vector Laboratories, Peterborough, UK) under glass cover slips. Mouse pancreatic sections were analyzed using a Leica DM5000 Epi-Fluorescent microscope and Leica Application Suite software.

MIN6 Cell culture and treatment

MIN6 beta-cells were cultured in DMEM media containing GlutaMAX, 25 mol/L glucose and Sodium pyruvate supplemented with 15% v/v foetal bovine serum, 1% v/v Penicillin/Streptomycin/Glutamine (all Life Technologies, Paisley, UK) and 5 µl β-mercaptoethanol. Cells were incubated for 48 h with recombinant eNAMPT (2 – 10 ng/ml; Adipogen, Seoul, South Korea) with or without eNAMPT-Ab (2.5 µg/ml). After 48 h treatments cells were analysed for changes in glucose-stimulated insulin secretion or NAD levels.

ESM Table

Tnfa	CGGAGTCCGGGCAGGT	GCTGGGTAGAGAATGGATGAACA
Il1b	GGGCTGCTTCCAAACCTTTG	TGATACTGCCTGCCTGAAGCTC
Il6	GGTGACAACCACGGCCTTCCC	ACAGGTCTGGGCTGCTGGTC
Adgre1	AGCACGTCCTATTICAACGGT	TCTGGAACACCACAAGAAAGTG
Ccl2	GGCTGGAGAGCTACAAGAGG	GGTCAGCACAGACCTCTCTG
Itgam	TGGACGCTGATGGCAATACC	GAGGCAAGGGACACACTGAC
Itgax	TGAGCTGTACCTGGATAGCCT	TGTGTCAGCTTCTCTGCATCC
Nampt	GCGAGCGAGCGGTGACT	CTGCGAGCAAGGAGAAAAATG
Puma	TTCATGGGACTCCTCCCCTC	GGTGTAGGCACCTAGTTGGG
Noxa	ACTGAACGGATGTTGCCTGT	CCCGGGGAAAAGATCACAGT
Bad	CTTGAGGAAGTCCGATCCCG	CATACTCTGGGCTGCTGGTC
Bax	GCTGGACACTGGACTTCCTC	GAGGCCTTCCCAGCCAC
Chop	CCTAGCTTGGCTGACAGAGG	GGGCACTGACCACTCTGTTT
Hmgb1	TTGCTTTGCCCATTTTGGGT	GGCATGTGGACAAAAGCTCTC
Srebf1	GCAGACCCTGGTGAGTGG	GTCGGTGGATGGGCAGTTT
Fasn	CACTGCATTGACGGCCGGGT	GGACAAGCCCAGGCTGCGAG
Dgat2	TCTCAGCCCTCCAAGACATC	GCCAGCCAGGTCAAGTAGAG
Pck1	TCCTGCAGAACACAAGGGC	GGTCGCATGGCAAAGGG

ESM Table 1. List of qRT-PCR primer sequences used in this study

ESM Figures and Legends

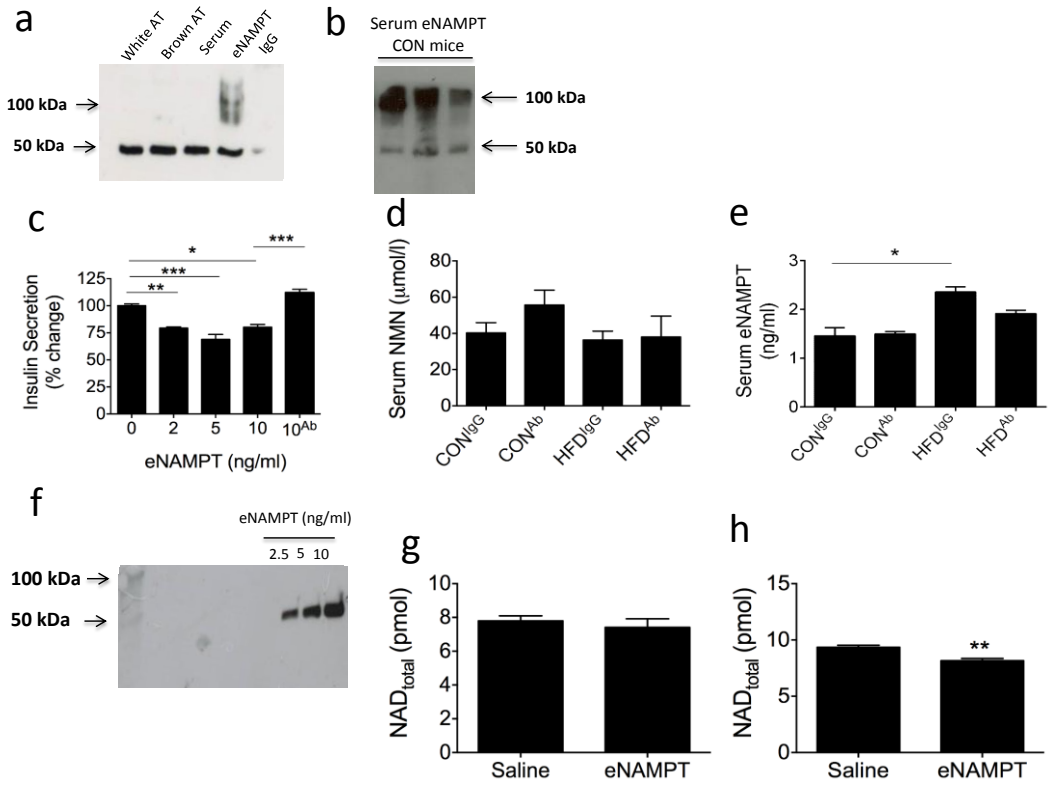

ESM Fig. 1. Specificity of eNAMPT-Ab and recombinant eNAMPT protein. (a) NAMPT/eNAMPT immunoprecipitation (with LSBio anti-NAMPT-Ab) and subsequent immunoblotting (with Bethyl Laboratories anti-NAMPT antibody); (b) serum eNAMPT monomer and dimer protein in CON fed mice, measured non-reducing SDS-PAGE and immunoblot (c) Glucose-stimulated insulin secretion from MIN6 cells following incubation with eNAMPT-monomer or co-incubated with eNAMPT-monomer and LSBio eNAMPT-Ab (48 h). Serum NMN (d) and total-eNAMPT (e) levels in 10 week-fed CON and HFD mice administered eNAMPT-Ab or control IgG. (f) Non-reducing SDS-PAGE gel and western blot of recombinant eNAMPT (Adipogen, Seoul, South Korea). NAD levels in (g) MIN6 cells following recombinant eNAMPT exposure (5 ng/ml; 48 h) and in (h) white AT following recombinant eNAMPT administration to mice (5 ng/ml/day; I.P. 14 days). Data are expressed as mean ± SEM. Statistically significant differences between groups are indicated by * p<0.05; ** p<0.01; *** p<0.001.

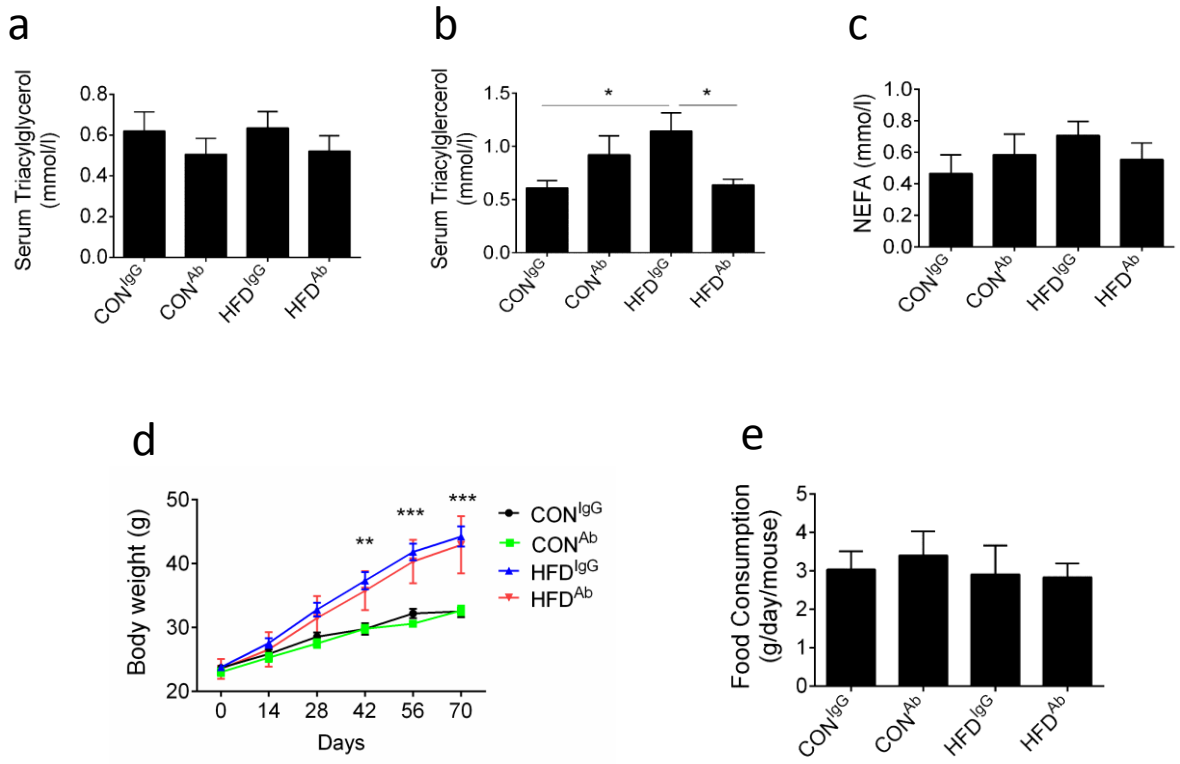

ESM Fig. 2. Effects of eNAMPT-Ab on body weight and serum lipids. CON and HFD mice (10 weeks) were administered eNAMPT-Ab or non-immune IgG; (a) Fasting serum triglyceride, (b) Fed serum triglyceride, (c) Fed serum NEFA levels, (d) Body weight, (e) Food intake post-antibody administration. Data are expressed as mean ± SEM. Statistically significant differences between are indicated by ** p<0.05; ** p<0.01; *** p<0.001;

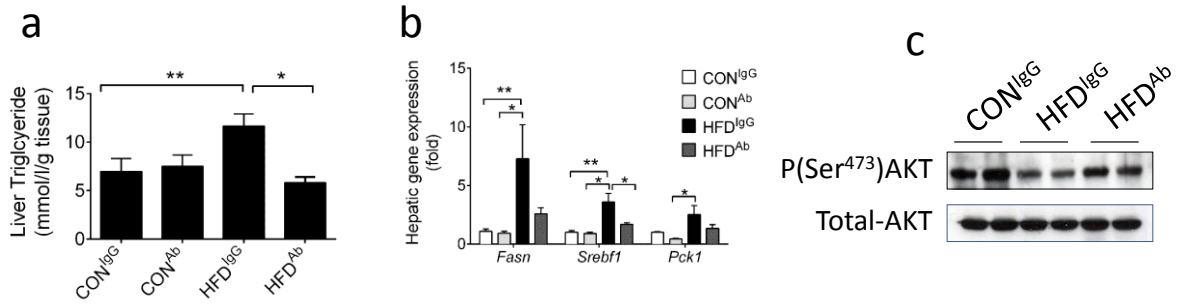

ESM Fig. 3. Effects of eNAMPT-Ab on liver insulin sensitivity and lipid levels. CON and HFD mice (10 weeks) were administered eNAMPT-Ab or non-immune IgG; (a) Liver triglycerides, (b) liver gluconeogenic and lipogenic gene expression, (c) liver phospho-AKT levels. Data are expressed as mean ± SEM. Statistically significant differences between groups are indicated by * $p<0.05$, ** $p<0.01$.

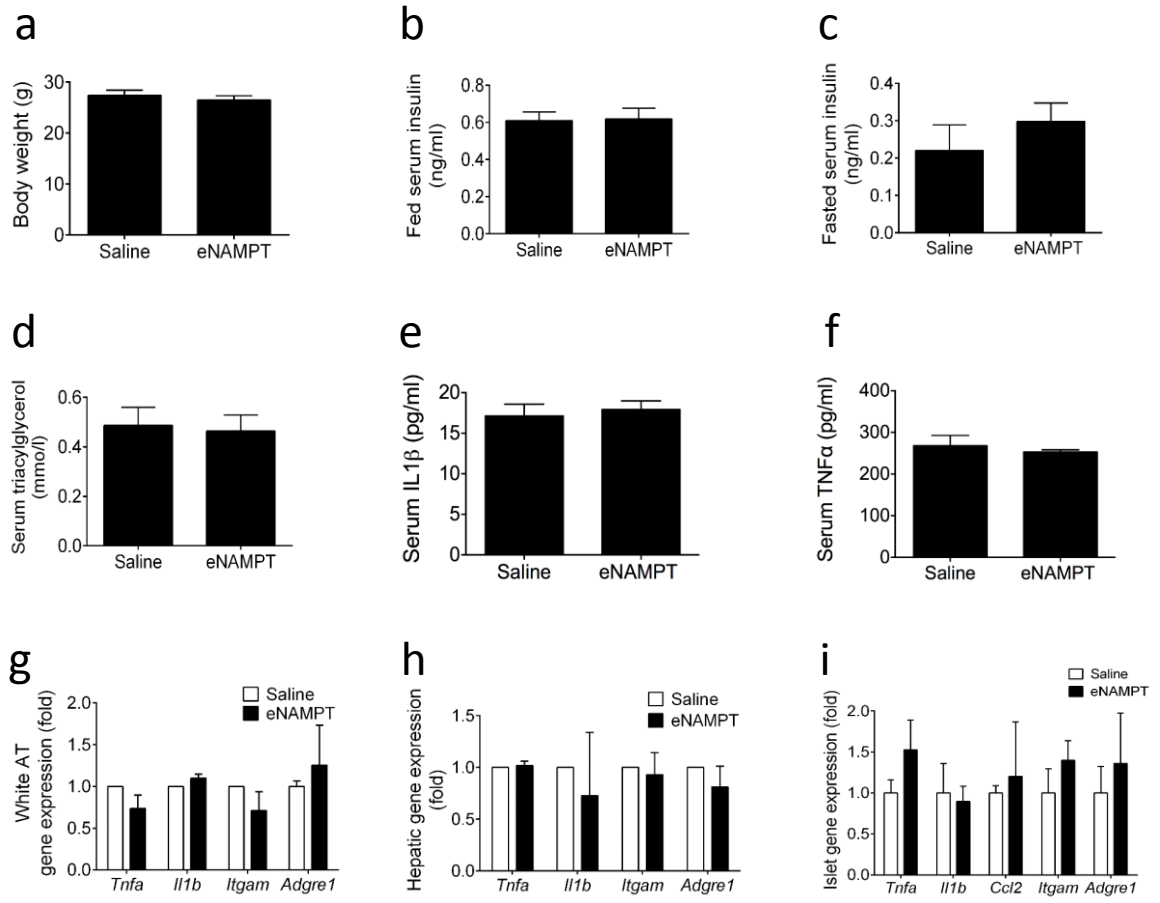

ESM Fig. 4. Effects of 14-day eNAMPT administration in mice. Mice were administered eNAMPT (5ng/ml) daily for 14 days; (a) body weight, (b) Fed serum insulin, (c) Fasting serum insulin (d) Serum Triglycerides, (e) Serum IL1β, (f) Serum TNFα. Pro-inflammatory gene expression in (g) WAT, (h) Liver, and (i) Islets. Data are expressed as mean ± SEM.

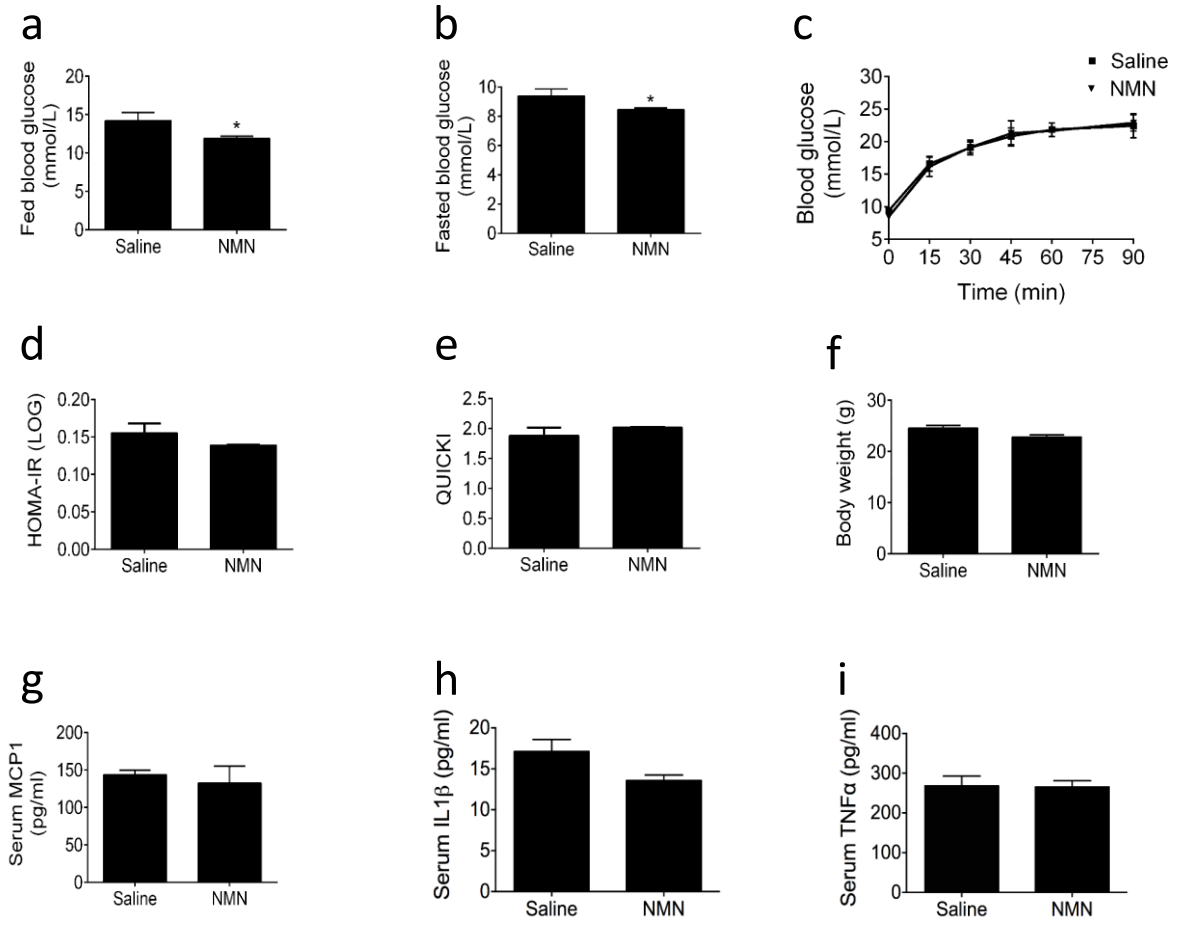

ESM Fig. 5. Effects of 14-day NMN administration in mice. Mice were administered NMN (500 mg/kg body weight) daily for 14 days; (a) Fed Blood Glucose, (b) Fasted blood glucose, (c) IPGTT; (d) HOMA-IR (LOG), (e) QUICKI; (f) Body weight. Serum levels of (g) MCP1, (h) IL1β and (i) TNFα. Data are expressed as mean ± SEM. Statistically significant differences between groups are indicated by * $p<0.05$.